

Exploring Binary Cesium-based Photocathode Materials via High-Throughput Density Functional Theory Calculations

Holger-Dietrich Saßnick¹ and Caterina Cocchi^{1,2}

¹Carl von Ossietzky Universität Oldenburg, Physics Department, 26129 Oldenburg

²Humboldt-Universität zu Berlin, Physics Department and IRIS Adlershof, 12489 Berlin

22nd September, 2022



Motivation and Goals

- ▶ Nowadays syntheses methods are still strongly relying on expensive trial-and-error approaches.
- ▶ Introduce a theoretical framework that gives insight into relationships between structural features and the material's properties.
- ▶ As a starting point we focus on "simple" binary systems that are well known and studied.

Experimental Collaborators



Prof. Dr. Thorsten Kamps,
Dr. Sonal Mistry
and team.



Dr. Sven Lederer
and team.



Bundesministerium
für Bildung
und Forschung



Niedersächsisches Ministerium
für Wissenschaft und Kultur

Sponsors

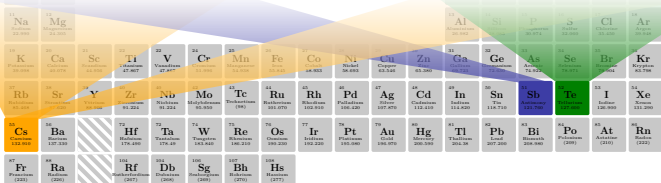
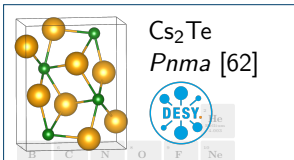


Project-id: 490940284



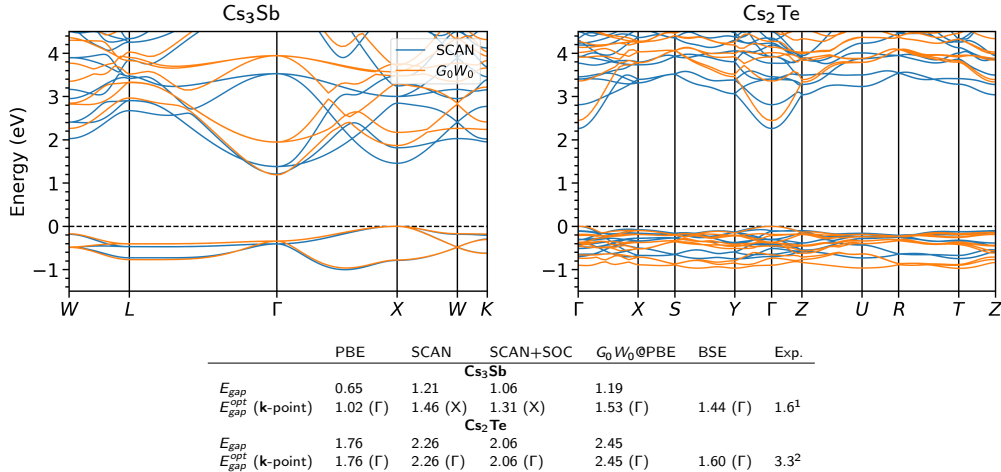
Project-id: nic00069

Ab-initio methods like density functional theory (DFT) allow the calculation of material's properties without empirical parameters.



57 La	58 Ce	59 Pr	60 Nd	61 Pm	62 Sm	63 Eu	64 Gd	65 Tb	66 Dy	67 Ho	68 Er	69 Tm	70 Yb	71 Lu
89 Ac	90 Th	91 Pa	92 U	93 Np	94 Pu	95 Am	96 Cm	97 Bk	98 Cf	99 Es	100 Fm	101 Md	102 No	103 Lr

Calculation results include electronic band structures



¹ Spicer, *Phys. Rev.* 1958, 112, 114–122; doi: 10.1103/PhysRev.112.114

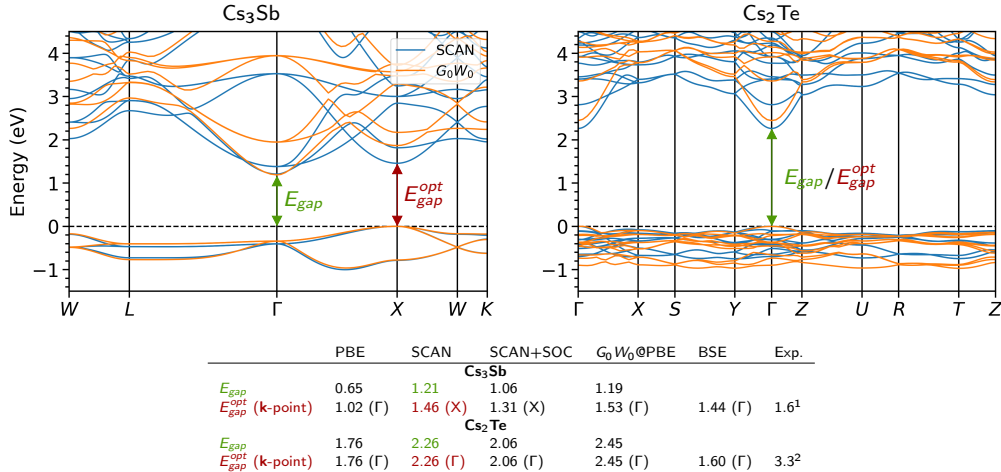
² Powell, Spicer, et al., *Phys. Rev. B* 1973, 8, 3987–3995; doi: 10.1103/PhysRevB.8.3987

Saßnick and Cocchi, *Electron. Struct.* 2021, 3, 027001; doi: 10.1088/2516-1075/abfb08

Cocchi and Saßnick, *Micromachines* 2021, 12(9), 1002; doi: 10.3390/mi12091002



Calculation results include electronic band structures



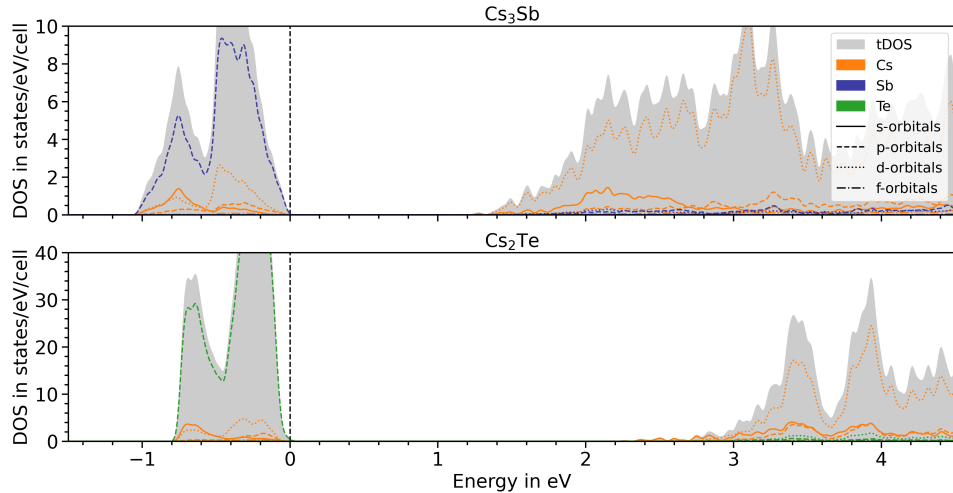
¹ Spicer, *Phys. Rev.* 1958, 112, 114–122; doi: 10.1103/PhysRev.112.114

² Powell, Spicer, et al., *Phys. Rev. B* 1973, 8, 3987–3995; doi: 10.1103/PhysRevB.8.3987

Saßnick and Cocchi, *Electron. Struct.* 2021, 3, 027001; doi: 10.1088/2516-1075/abfb08

Cocchi and Saßnick, *Micromachines* 2021, 12(9), 1002; doi: 10.3390/mi12091002

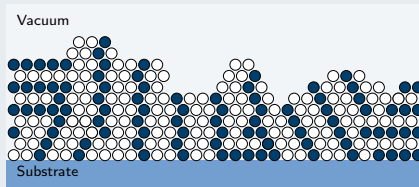
And the projected density of states of the electrons



High-throughput methods and their benefits

Better insight into microstructure

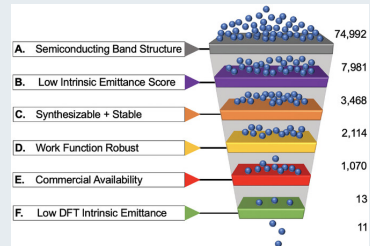
Synthesis route via PVD results in polycrystalline materials:



By restricting the screening space to a binary system, crystal structures that are likely to form during the syntheses process can be theoretically calculated.

Identifying novel materials

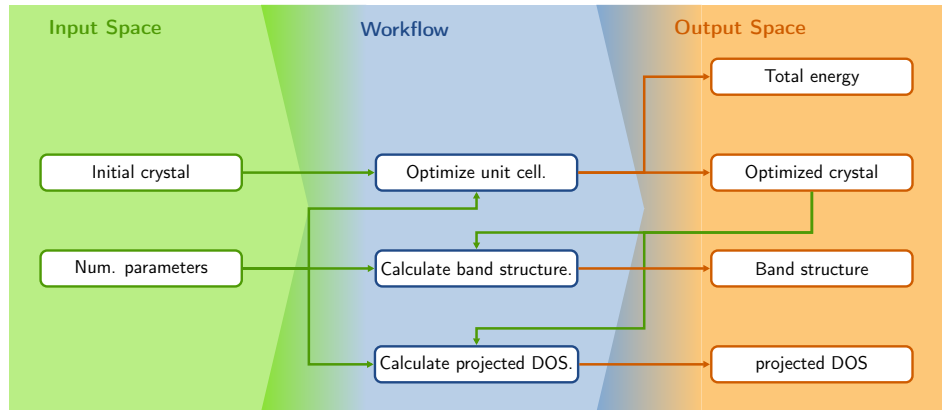
synthesis and experimental analysis of a large manifold of materials is very expensive.



Screening of a manifold of different material classes to check suitability for the application.

Antoniuk, Schindler, et al., *Adv. Mater.* 2021, 2104081;
doi: 10.1002/adma.202104081

The technical implementation of a high-throughput workflow



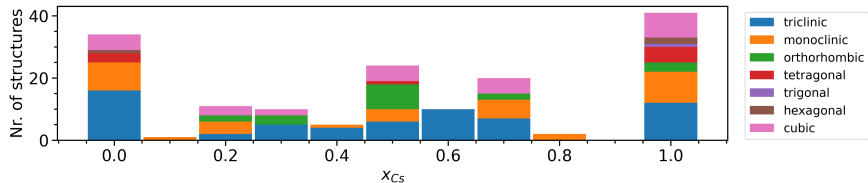
- ▶ The high-throughput workflow has been designed using AiiDA.

Huber, Zoupanos *et al.*, *Scientific Data* 2020, 7, 300; doi: 10.1016/j.commatsci.2020.110086

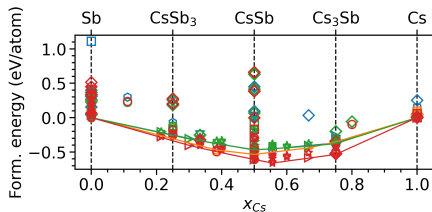
Uhrin, Huber *et al.*, *Comp. Mat. Sci.* 2021, 187; doi: 10.1016/j.commatsci.2020.110086

The Cs-Sb system

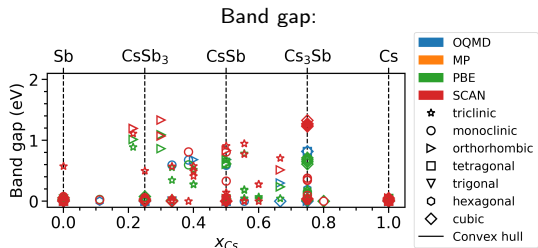
Distribution of the crystal structures:



Stability:



Band gap:

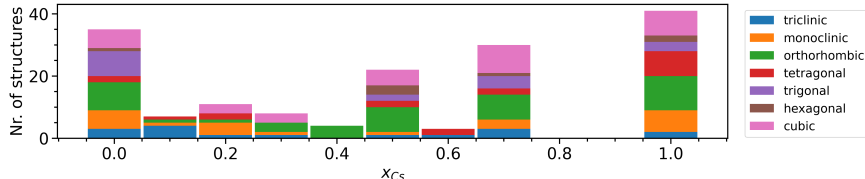


► $E_{form}(Cs_xSb_{1-x}) = E(Cs_xSb_{1-x}) - [xE(Cs) + (1-x)E(Sb)]$

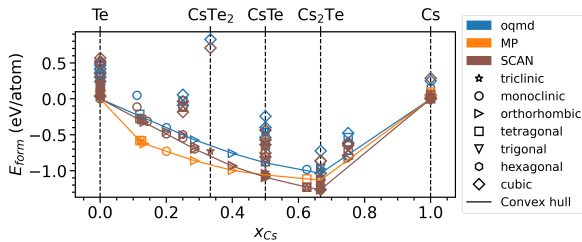
Cocchi and Saßnick, *Micromachines* 2021, 12(9), 1002; doi: 10.3390/mi12091002

The Cs-Te system

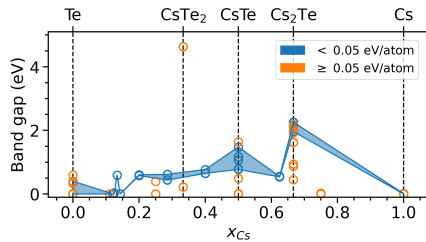
Distribution of the crystal structures:



Stability:

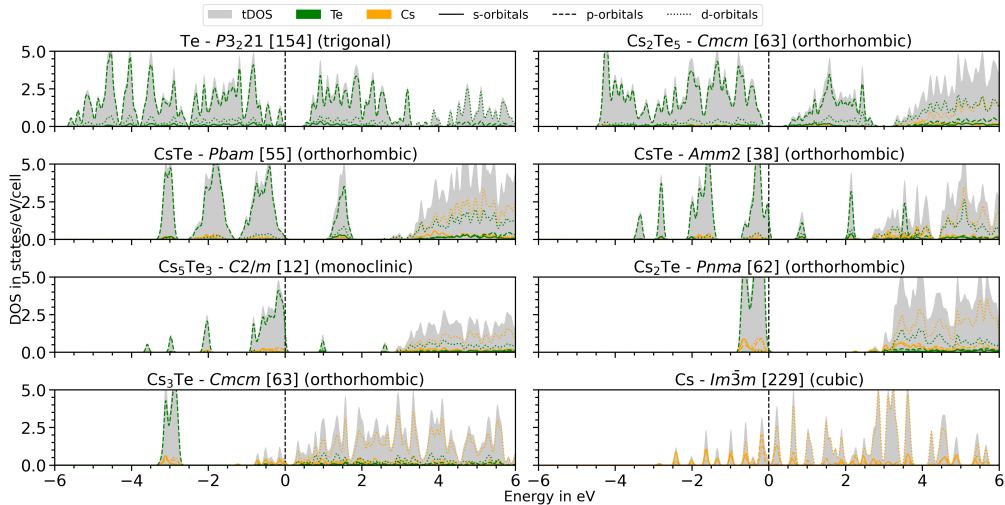


Band gap:



► $E_{\text{form}}(\text{Cs}_x \text{Te}_{1-x}) = E(\text{Cs}_x \text{Te}_{1-x}) - [xE(\text{Cs}) + (1-x)E(\text{Te})]$
 Saßnick and Cocchi, J. Chem. Phys. 2022, 156, 104108; doi: 10.1063/5.0082710

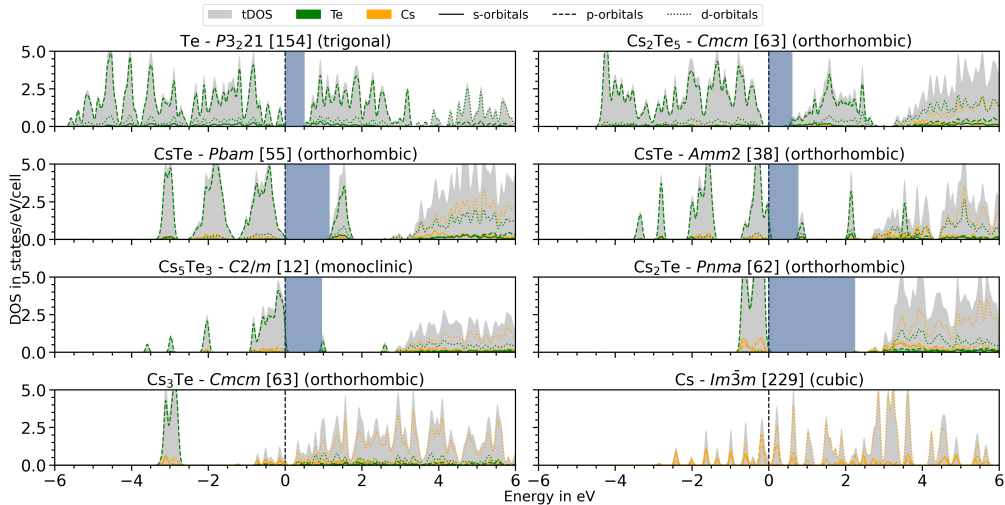
Changing electronic character with composition



0 eV is set to the valence band maximum (VBM).

Saßnick and Cocchi, *J. Chem. Phys.* 2022, 156, 104108; doi: 10.1063/5.0082710

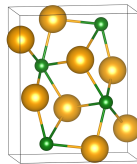
Changing electronic character with composition



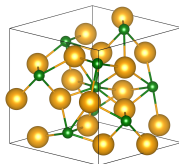
Most stable phases with the experimental composition of 2:1 (1)

- ▶ 10 different crystals have a distance to convex hull smaller than 0.05 eV/atom.
- ▶ Based on their structural similarity 4 groups can be distinguished.
- ▶ For the latter calculations only the structure with the highest symmetry is considered:

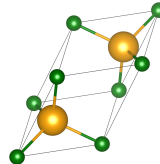
Pnma [62] (orthorhombic)



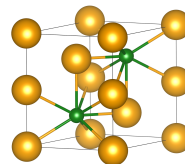
R3 [146] (trigonal)



Fm $\bar{3}m$ [225] (cubic)

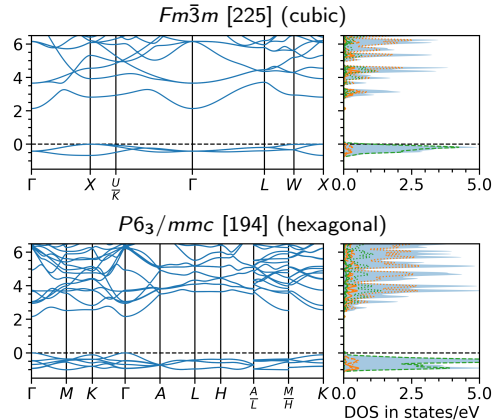
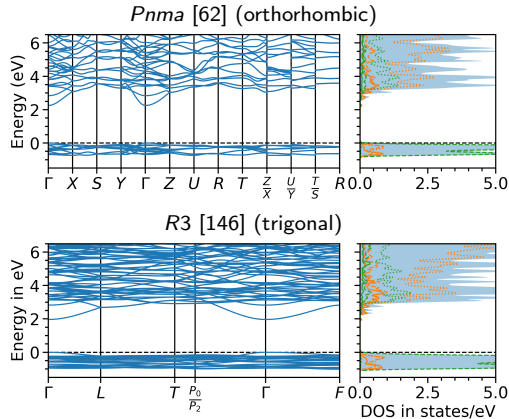


P6₃/mmc [194] (hexagonal)



● Cs ● Te

Most stable phases with the experimental composition of 2:1 (2)



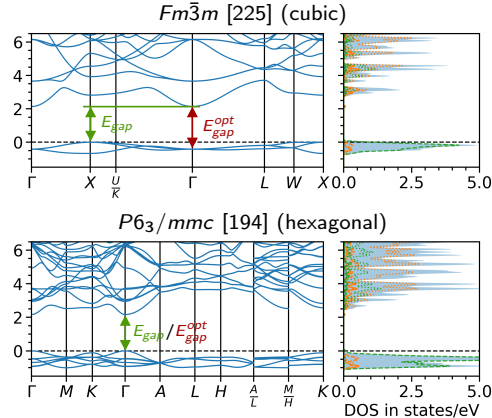
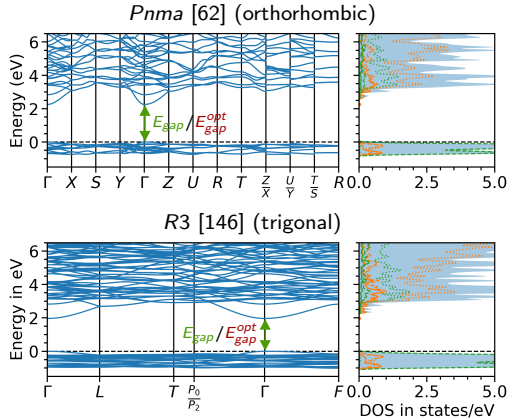
	<i>Pnma</i> [62]	<i>Fm$\bar{3}m$</i> [225]	<i>R3</i> [146]	<i>P6₃/mmc [194]</i>
E_{gap} in eV (k-points)	2.25	2.14 ($X \rightarrow \Gamma$)	1.96	2.16
E_{gap}^{opt} in eV (k-point)	2.25 (Γ)	2.55 (Γ)	1.96 (Γ)	2.16 (Γ)

0 eV is set to the valence band maximum (VBM).

Saßnick and Cocchi, *J. Chem. Phys.* 2022, 156, 104108; doi: 10.1063/5.0082710



Most stable phases with the experimental composition of 2:1 (2)

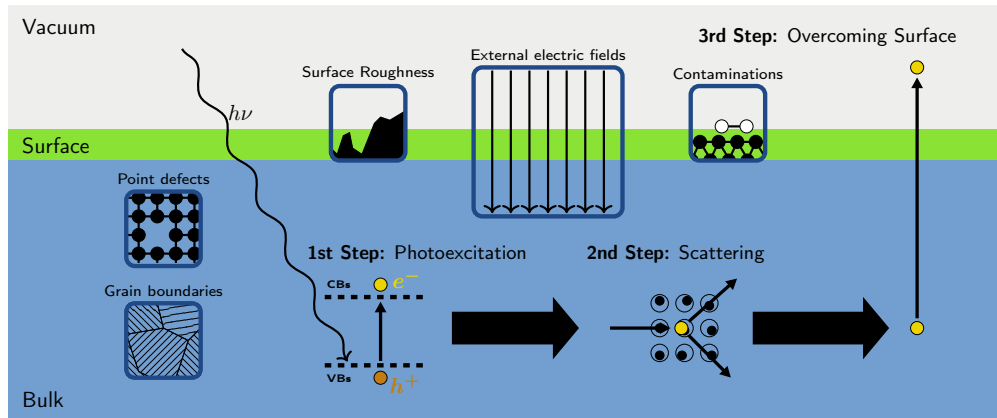


	<i>Pnma</i> [62]	<i>Fm$\bar{3}m$</i> [225]	<i>R3</i> [146]	<i>P6₃/mmc [194]</i>
E_{gap} in eV (<i>k</i> -points)	2.25	2.14 ($X \rightarrow \Gamma$)	1.96	2.16
E_{gap}^{opt} in eV (<i>k</i> -point)	2.25 (Γ)	2.55 (Γ)	1.96 (Γ)	2.16 (Γ)

0 eV is set to the valence band maximum (VBM).

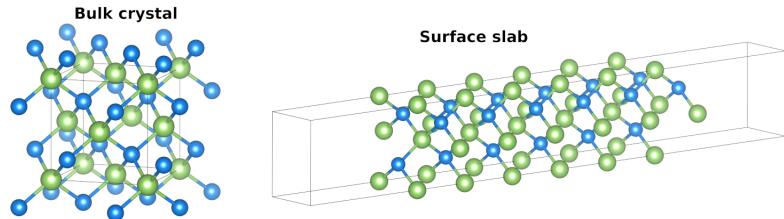
Saßnick and Cocchi, *J. Chem. Phys.* 2022, 156, 104108; doi: 10.1063/5.0082710

The role of surfaces in the photoemission process

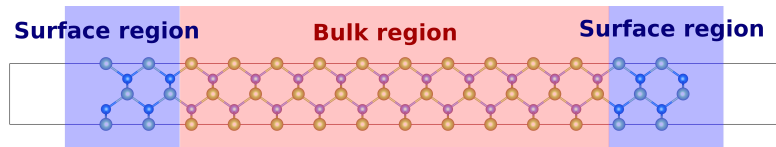


How to model a surface?

The surface breaks the periodicity in one dimension, thus making it necessary to treat this direction with non-periodic boundary conditions:

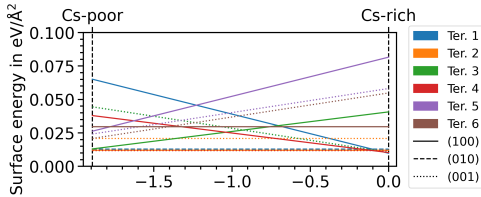


resulting in slabs which contain two surface facets:

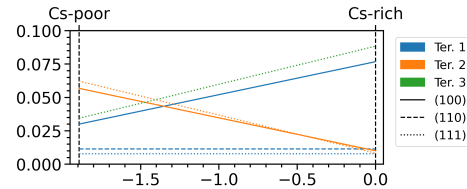


Surface Stability

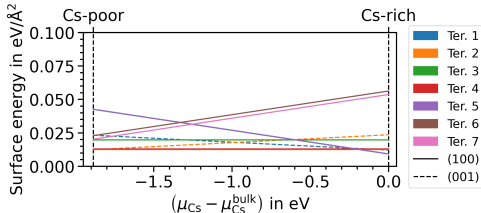
Cs_8Te_4 [62] $Pmna$ (orthorhombic)



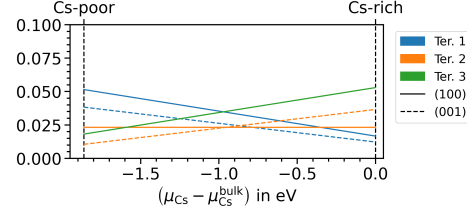
Cs_2Te_1 [225] $Fm\bar{3}m$ (cubic)



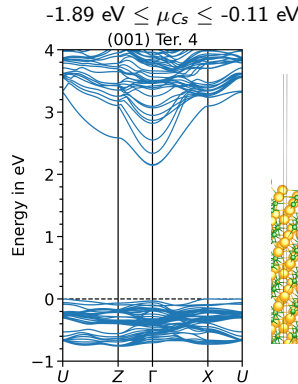
$\text{Cs}_{18}\text{Te}_9$ [146] $R3$ (trigonal)



Cs_4Te_2 [194] $P6_3/mmc$ (hexagonal)

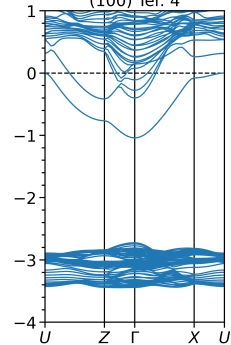


Surface properties of the Cs_8Te_4 [62] $Pmna$ phase

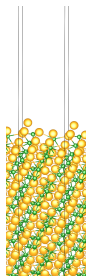
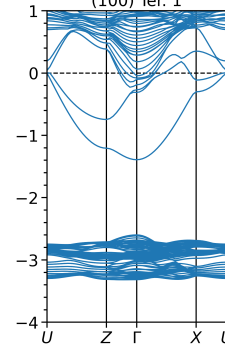


$Cs\text{-poor} \longrightarrow Cs\text{-rich}$

$-0.11 \text{ eV} \leq \mu_{Cs} \leq -0.03 \text{ eV}$
 (100) Ter. 4



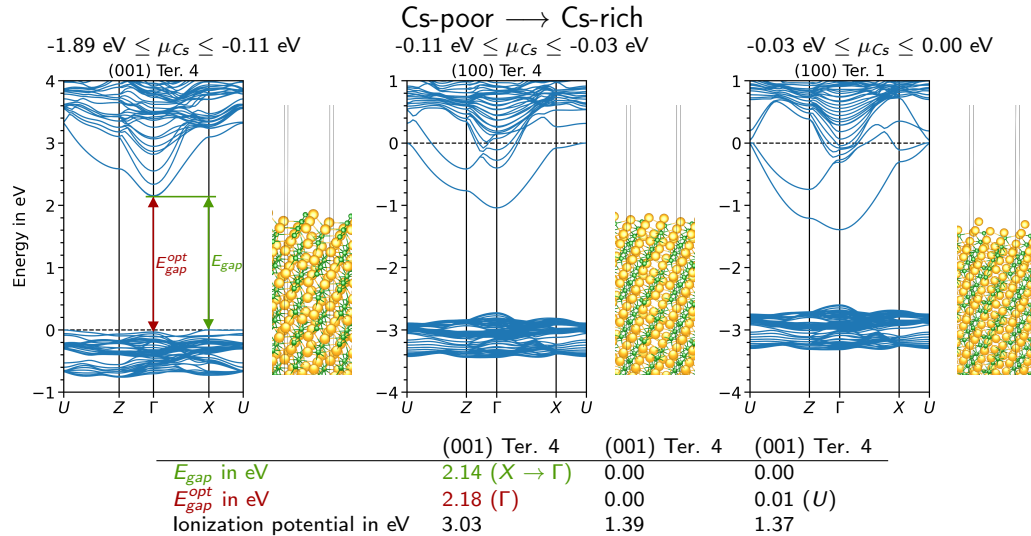
$-0.03 \text{ eV} \leq \mu_{Cs} \leq 0.00 \text{ eV}$
 (100) Ter. 1



	(001) Ter. 4	(001) Ter. 4	(001) Ter. 4
E_{gap} in eV	2.14 ($X \rightarrow \Gamma$)	0.00	0.00
E_{gap}^{opt} in eV	2.18 (Γ)	0.00	0.01 (U)
Ionization potential in eV	3.03	1.39	1.37

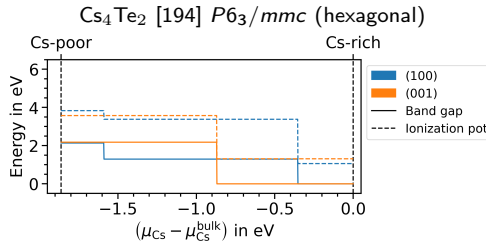
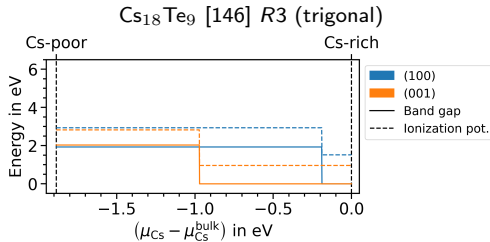
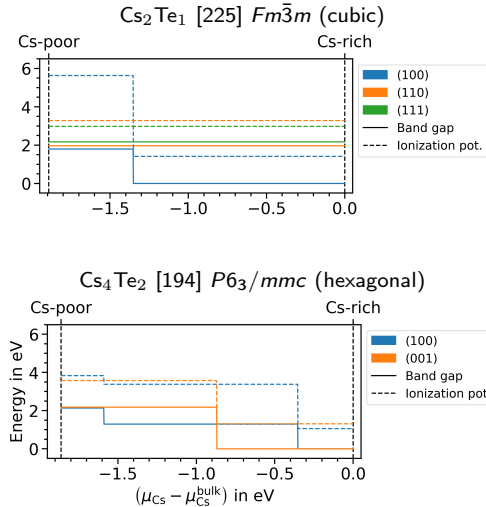
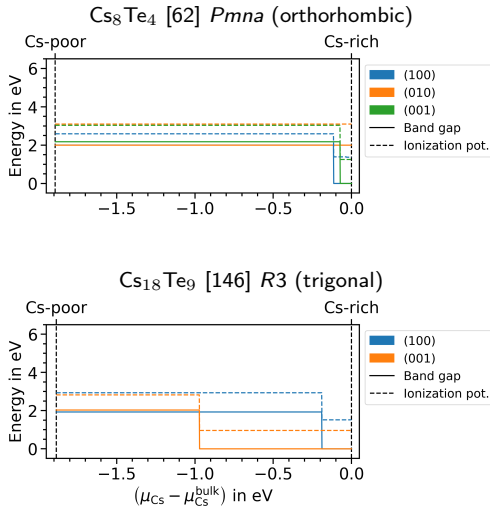
0 eV is set to the valence band maximum (VBM).
 Saßnick and Cocchi, *in preparation*.

Surface properties of the Cs_8Te_4 [62] $Pmna$ phase



0 eV is set to the valence band maximum (VBM).
 Saßnick and Cocchi, *in preparation*.

Overview of the electronic properties of all surface facets





Conclusions

- ▶ First approximation of the stability of different bulk phases and surface facets.
- ▶ Analysis of relationship between compositional changes and electronic properties.
- ▶ Additional (theoretically) stable structures found at experimentally relevant compositions.
- ▶ The largest band gap is reached at a composition of 2:1 due to fully occupied Te p-states for Cs-Te.
- ▶ Surface facets tend towards metallic properties in Cs-rich environments accompanied with a reduction in the ionization potential.
- ▶ The routine can be applied to any material-system and we are planning to publish the source code soon.